The Severe Depletion of Turbulent Echo Power in association with Precipitation observed by Using Chung-Li VHF Radar

Yen-Hsyang Chu and Chun-Hsien Lin

Institute of Space Science, NCU, Chung-Li, Taiwan, R.O.C.

Abstract

According to the earlier observations of precipitating atmosphere by using various VHF radars, it shows that the VHF radar echo powers scattered from precipitation particles are generally much weaker than those scattered from refractivity fluctuations by about 20-30 dB occurred below the level of melting layer. However, in this article, it is first time to demonstrate that the precipitation echo powers occurred within the height range from about 2.5 km to 5 km, which is below the level of 0° C isotherm, may be far exceeded than the turbulent echo powers by about 15 dB observed by Chung-Li VHF radar. After examining the echo power profiles of the precipitations and refractivity fluctuations in more detail, it reveals that this feature can be attributed to abnormally severe depletion of turbulent echo power associated with quite intense upward air motion. Further analysis indicates that the correlation between hydrometeor terminal velocity and precipitation echo power is positive, while anti-correlation is found between vertical wind velocity and turbulent echo power. Based on these observational results, a scenario is proposed in order to explain the cause of abnormal depletion of refractivity echo power.

1. Introduction

During the period of last two decades, VHF radar has been proved to be a very powerful ground based instrument employed for background atmospheric observations. A number of important atmospheric parameters, such as 3-dimensional wind field, tropopause height, vertical wind shear, turbulent strength, aspect sensitivity, tropo- and lower stratospheric temperature profile in compliance with RASS, etc., have been measured successfully with VHF radar by various investigators (Balsley and Gage, 1980; Gage et al. 1986; Masuda, 1988; Woodman and Chu, 1989). In recent years, moreover, it is also shown that VHF radar has the great potential of atmospheric precipitation measurements. For example, Fukao et al.(1985) presented the observational results of precipitating atmosphere and obtained the terminal velocity of rain drops in the cold front with MU VHF radar. Wakasugi et al.(1986,1987) deduced the size distribution of rain drops from the Doppler spectra of precipitation returns obtained by MU VHF radar. Larsen and Rottger (1987) reported the observations of precipitations within the thunderstorm with SOUSY VHF radar. Chu et al.(1991) observed the salient bright band structure and some other interesting features associated with typhoon precipitation by using Chung-Li VHF radar. All of these investigations indicate that VHF radar indeed can be employed for precipitation measurement.

According to the earlier observations (Fukao et al., 1985; Wakasugi et al., 1985; Larsen and Rottger, 1987; Chu et al., 1991), outside the bright band structure, the VHF radar echo powers originated from precipitation particles are generally much weaker than those from atmospheric refractivity fluctuations by about 15-30 dB. While in the melting layer, the former may be comparable to or slightly stronger than latter by 3-5 dB. Since the turbulent echo signals dominate the VHF radar returns in most part of precipitating atmosphere, it is reasonable that the precipitation echoes may be generally ignored during the VHF radar signal processing for background atmospheric parameters estimation. However, in a specific precipitating environment, if the echo powers of precipitations are so intense that they are comparable to or even stronger than those of turbulences, it can be expected that neglecting the precipitation echo signals will cause significant error on the induction of atmospheric parameters. In this article, the observational results that the VHF radar echo powers scattered from hydrometeors of Mai-Yu front below the level of melting layer may be considerably larger than those from refractivity fluctuations by about 15 dB will be presented and discussed. In section two, the characteristics of Chung-Li VHF radar will be introduced briefly. In section three, the results of the depletion of the turbulent echo powers, which correspond to the feature of precipitation echo powers being greater than turbulent echo powers occurred below the height of 0° isotherm, will be shown and analyzed detailedly. The relations between several specific parameters induced from the observed Doppler spectra , e.g., vertical wind velocity, terminal speed of hydrometeor, echo power of turbulent and precipitation, will be investigated in section four. According to the observational results, a scenario will be proposed in this section in order to explain the behavior of abnormal degradation of turbulent echo power. The conclusion will be given in section five.

2. Chung-Li VHF radar

Chung-Li VHF radar is located at the campus of National Central University in Taiwan , Republic of China. This radar is consist of three independent and identical modules. Each antenna module is a square array with 64 Yagi antenna elements (8X8). The whole antenna is arranged as an equal lateral triangle with length 45, 45, and 40 m, respectively, and the apex is pointed toward north by west 22.3°. The total physical antenna area is 4800 m^2 (3X40X40). The operational frequency is 52 MHz (corresponding to 5.77 m wavelength) and the peak transmitted power is 180 kw (3X60). The maximum duty cycle is 2%, and the pulse width can be set from 1 μs to 999 μs. The antenna beam width for each module is 7.4° and 5° for whole array. The radar beams can be pointed not only toward zenith, but also toward northwest, northeast, southeast and southwest with fixed zenith angle 17°. For more informations about Chung-Li VHF radar, the reference of Rottger et al. (1990) could be

referred.

3. Observations

The Chung-Li VHF radar data analyzed in this study were taken on April 20, 1988, from 0856LT to 1035LT. During this period, a Mei-Yu front was passing through the Taiwan area and moving toward northwest. According to the measurement of the meteorological station located in the campus of National Central University, the amount of the rainfall occurred from 08LT to 20LT is 66.5 mm. The radar parameters used for this study were set as follows: pulse width 2 μs, coherent integration time 0.2 s, inter-pulse period 200 μs, and the starting altitude was 1.8 km, with 40 range gates recorded. The three independent radar beams were steered simultaneously toward zenith, northwest, and northeast, respectively. The Doppler spectra are calculated by using 64 points FFT algorithm. The echo power, mean Doppler frequency shift and spectral width for the precipitation particles and the atmospheric refractivity fluctuations are estimated with the least square method, in which the Gaussian curve is employed to fit the corresponding observed Doppler spectrum.

Fig.1a displays the shade plots of Doppler spectra averaged over 2.1 minutes for different three radar beams observed around 0910LT, 20 April 1988. As indicated, below about 5 km two remarkable spectral peaks can be discriminated clearly. One of the peaks is appeared in the spectral region close to zero Doppler frequency shift and changes its position unevenly with height. While the other spectral peak is always located in the spectral range with negative radial velocity (i.e., positive Doppler frequency shift) and shifted abruptly toward center of spectrum above the height around 4 km. According to Pan-Chiaou rawinsonde data (departed from Chung-Li VHF radar station about 25 km northeast) measured at 08LT, the level of 0° C isotherm (i.e., melting layer) is located at the altitude of 4.2 km. According to the informations given above and the results obtained by earlier works on the investigations of precipitating environment, it can be realized that the former spectral peak is originated from precipitation scatters and the latter one is generated from refractivity fluctuations. Examining Fig.1a in more detail, it can be found that the turbulent echo power is maximum between 3.5 km to 4.5 km and its value is far exceeded than precipitation echo power by about 20 dB. Therefore, at this instant, the turbulent echoes dominate the VHF returns. However, this situation is totally reversed just 17 minutes after. Fig.1b is the shade plot same as Fig.1a, but taken at 0927LT. It shows that two salient spectral peaks, one corresponds for precipitation echoes and the other one is responsible for refractivity returns, can also be observed in this sketch as same as Fig.1a. After comparing with Fig.1a, it reveals that the strength and the height variation of the precipitation echo power shown in Fig.1b differ not too much from those shown in Fig.1a, however, the significant changes are occurred on the height distribution of turbulent echo powers displayed in Fig.1b. As indicated, the locations of the maximum turbulent echo powers for three independent radar beams are shifted coherently down to the height around 2.5 km. Moreover, the echo powers of precipitation are greater than those of refractivity fluctuations by the amount up to 15 dB over the height range from 3.8 km to 4.5 km due to the severe depletion of turbulent echo powers. It should be noted that the feature of degradation of turbulent echoes in precipitating environment will affect considerably the accuracy of background wind estimation if the precipitation and turbulent echo signals are not separated from received VHF radar returns and processed independently during the procedure of VHF radar signal analysis.

In order to compare the relative changes between the echo power profiles of precipitation and those of refractivity fluctuations , the successive variations of echo power profiles with time are plotted respectively for different radar means and shown in Fig.2, where the dotted and solid lines represent the profiles of precipitation and turbulence, respectively. Notice that the echo power profiles for vertical pointed radar beam are discarded after 0943LT because of the radar system interference. Investigating Fig.2 detailedly, it can be found that before 0900LT the turbulent echo powers are comparable to or slightly higher than precipitation echo powers, but between 0900LT and 0923LT the turbulent echo powers are stronger than the precipitation echo powers through the overall height range, whereas after 0925LT the turbulent echo powers are depleted enormously within 3 km to 4.5 km altitude range such that the precipitation echo powers are superior to the turbulent echo powers. Moreover, after examining the echo power profiles of precipitation shown in Fig.2 more detailedly, it displays that for vertically pointed radar mean the slight bright band structures are occurred during the period from 0900LT to 0928LT, while no bright band structures can be observed before 0900LT and after 0928LT. This feature can also be found on the profiles of oblique radar beams, although a little differences are existed between them. From these observationnal results, it shows that the occurrence of turbulent echo power depletion seems to match with that of bright band vanish. In the following section, the physical mechanism that is related to the disappearance of bright band structure and causes the severe depletion of turbulent echo powers in the precipitating atmosphere will be proposed and discussed.

4. Results and Discussion

In previous section, it has been shown that the severe depletion of turbulent air reflectivity may occur below the level of melting layer in precipitating atmosphere. This feature addresses the important question: what is the physical mechanism to initiate this phenomenon. Before answering this question, the following analyses are necessary. Fig.3 shows the height-time variation of vertical air velocity estimated from Doppler spectral components of refractivity echoes. As indicated, fairly intense updrafts with velocities ranging from 3 m/s up to 5 m/s are occurred during the periods before 09LT and after 0925LT. Referring to Fig.2, the occurrence of these strong updrafts seems to coincide with the vanish of bright band structures. In fact, Szoke and Zipser (1986) has pointed out that one of the necessary conditions for the formation of bright band is that the vertical air velocity should be less than the fall speed of melting snow particles, i.e., about 2 m/s (Battan, 1973; Chu et al., 1991). Examining the distribution of vertical wind velocity presented in Fig.3, it indicates that no vertical speed exceeded 2 m/s can be observed during the period from 0900LT to 0925LT, quite consistent with the formation of bright band as shown in Fig.2. Additionally, it also shows that the depletion of turbulent echo powers seems to be closely related to the occurrence of intense updraft. In order to find out their relationship, the comparison of the temporal variation of vertical air velocities with those of turbulent echo powers is made and shown in Fig.4, where the solid and dash-dotted lines represent respectively the time series of vertical turbulent echo power and those of vertical air velocity. As indicated, it is quite evident that high anti-correlation between these two series can be observed , especially over the height range from 3 km to 5 km with averaged correlation coefficient of -0.82. This feature strongly suggests that the depletion of turbulent echo powers is closely correlated to atmospheric dynamics. Fig.5 displays the comparison of temporal variations of hydrometeor terminal velocity with those of precipitation echo power, where solid line represents the hydrometeor terminal velocity, while dash-dotted line is the precipitation echo power. From Fig.5, it is very clear that hydrometeor terminal velocity positively correlates very well to precipitation reflectivity, quite consistent with the theoretical prediction of hydrometeor echo mechanism through Rayleigh scattering (Atlas et al., 1973; Battan, 1973). Additionally, the relationship between the air vertical velocity and hydrometeor terminal velocity is also analyzed and shown in Fig.6, where each dot in the plot is the spatial average over the height range from 3 km to 5 km. It can be seen that the correlation between air vertical velocity and hydrometeor terminal speed is highly positive, with a

correlation coefficient of 0.78. Making use of the results obtained in Fig.4, 5 and 6, the correlation between echo power of hydrometeor and that of refractivity fluctuation can be expected to be negative.

Based on the previous analysis, a scenario that can explain the behavior of depletion of turbulent echo power associated with strong updraft in precipitation environment will be proposed as follows. It is well-known that the refractive index of neutral atmosphere, n, can be expressed in terms of atmospheric pressure P, temperature T and water vapor pressure e and is given approximately as follows (Bean and Dutton, 1966)

$$n = 1 + (\frac{77.6}{T}(P + \frac{4810e}{T}))x10^{-6} \quad (1)$$

According to the theory of EM wave propagating through random medium (Tatarskii, 1961), the radar reflectivity originated from atmospheric refractivity fluctuations is anticipated to be proportional to the variance of atmospheric refractive index fluctuations, $<\Delta n^2>$. Following the derivation of Gossard and Strauch (1983), $<\Delta n^2>$ can be expressed mathematically as

$$<\Delta n^2>x10^{12} = A<\Delta P^2> + B<\Delta T^2> + C<\Delta q^2> + D<\Delta T\Delta P> + E<\Delta q\Delta P> + F<\Delta T\Delta q> \quad (2)$$

$$A = (\frac{77.6}{T} + \frac{600q}{T^2})2 \quad (3)$$

$$B = (\frac{77.6P}{T^2} + \frac{1200Pq}{T^3})2 \quad (4)$$

$$C = \frac{360000P^2}{T^4} \quad (5)$$

$$D = -2(\frac{77.6}{T} + \frac{600q}{T^2})(\frac{77.6P}{T^2} + \frac{1200Pq}{T^3}) \quad (6)$$

$$E = 2(\frac{77.6}{T} + \frac{600q}{T^2})\frac{600P}{T^2} \quad (7)$$

$$F = -2(\frac{77.6P}{T^2} + \frac{1200Pq}{T^3})\frac{600P}{T^2} \quad (8)$$

where the water vapor pressure has been replaced by mixing ratio q. Referring to Fig.1b and 2, it demonstrates that the depletion of turbulent echo powers is primarily occurred over the height range from 4.5 km to 3 km. In order to realize the weighting of each term on the variance of Δn, by using the rawinsonde data of Pan-Chiaou station around the height of 4.3 km launched at 08LT, substituting the average values of T=-0.5$_\circ$, P=630 mb, and q=5.4 g/kg into equation (3) - (8), equation (2) can then be represented numerically as follows

$$<\Delta n^2>x10^{12} = 0.108<\Delta P^2> + 0.739<\Delta T^2> + 25.91<\Delta q^2> - 0.566<\Delta T\Delta P> + 3.35<\Delta q\Delta P> - 8.756<\Delta T\Delta q> \quad (9)$$

From equation (9), it shows that not only the variance of pressure, temperature and mixing ratio will contribute to the magnitude of $<\Delta n^2>$, but also the covariance of these atmospheric parameters do. Because the variation of atmospheric pressure seldom exceeds 0.01 mb and the magnitude of $<\Delta T^2>$ and $<\Delta q^2>$ are comparable to each other, after comparing the weighting of each term in equation (9) on $<\Delta n^2>$, it is quite clear that the variance of Δq and the covariance of Δq and ΔT are two major terms that dominate significantly the magnitude of $<\Delta n^2>$. Notice that a minus sign appears before the term of $<\Delta T\Delta q>$, hence $<\Delta n^2>$ will be increased if the covariance of Δq and ΔT is negative, and vice versa. Namely, the radar echo power of refractivity fluctuations will be weakened if temperature-humidity covariance $<\Delta T\Delta q>$ is positive, and that will be enhanced if $<\Delta T\Delta q>$ is negative (Gossard and strauch, 1983). There are several atmospheric thermodynamic processes that may affect the sign of $<\Delta T\Delta q>$. For example, turbulent mixing process in the unsaturated environment with large vertical humidity gradient will cause $<\Delta T\Delta q>$ to be negative if air parcel is moved adiabatically and no water vapor condensation is occurred. This process has been applied by Wakasugi et al. (1987) to interpret the enhancement of turbulent echo power observed above the melting layer. The evaporation (or condensation) effect on rest hydrometeor will also give rise to negative covariance of ΔT and Δq due to the absorption (or release) of latent heat and increase (or decrease) of mixing ratio. However, the condensation effect of water vapor associated with strong updraft in saturated environment will be responsible for positive temperature-humidity covariance. This effect can be illustrated as follows. In precipitating atmosphere, the updraft will lift up a moist air parcel saturated-adiabatically. Because of the effect of the adiabatic cooling on the ascending air parcel, the water vapor will be condensed into liquid water droplet and the mixing ratio will be decreased if the condition of supersaturation is reached. The stronger the updraft is, the higher the air parcel can be lifted up, and the lower the mixing ratio will be. Nevertheless, during the thermodynamic process of water vapor condensation, the latent heat will be released to the air parcel. It implies that if this heating effect is competitive to the adiabatic cooling effect, the sign of temperature-humidity covariance will no longer be positive. After comparing the amount of latent heat released due to condensation with that of internal energy decreased due to adiabatic cooling, it shows that the former is only several percentage (in general less than 5%) of the latter in the case of moderate precipitation (Wallace and Hobbs, 1977). Consequently, the heating effect on the air parcel resulted from water vapor condensation can be neglected in this experiment. Under these considerations, the positive correlation between the variation of temperature and mixing ratio can be expected. That is , the radar reflectivity of refractivity fluctuations will be diminished. Based on previous inference, the correlation between vertical wind velocity and turbulent echo power will be anticipated to be negative, and the observations are shown in Fig.4. Additionally, once the condensation of water vapor is taking place, the number of precipitation particles and the size of the hydrometeors, which both contribute to the radar reflectivity of precipitation as predicted by the theory of Rayleigh scattering (Battan, 1973), are increasing simultaneously through the processes of water vapor attachment on atmospheric aerosols and droplet coalescence, respectively (Fletcher, 1972). Since the terminal velocity of precipitation particle is proportional to the size of hydrometeor up to about 0.5 cm (Atlas et al., 1973; Doviak and Zrnic, 1984), it is straightforward that precipitation echo power will be proportional to hydrometeor terminal velocity, as exhibited in Fig.5. Noting that the higher the humid air parcel is lifted up by the strong updraft, the lower the mixing ratio will be due to the water vapor condensation, as illustrated before. Subsequently, the size of hydrometeor will become larger and larger through the coalescence of droplets. Under these circumstances, the feature of positive correlation between air vertical speed and hydrometeor terminal velocity will be anticipated, as shown in Fig.6. From the previous discussions and observations, it is concluded that the depletion of turbulent echo power in the precipitating environment is indeed caused by the effects of mixing ratio decreasing and adiabatic cooling of air parcel associated with the strong updraft.

5. Conclusion

In this paper, the results of high-temporal precipitation measurements with Chung-Li VHF radar during the passage of Mei-Yu front on April 20, 1988, are presented and discussed. Usually, the echo powers from precipitation

scatterers are smaller than those from atmospheric refractivity fluctuations. However, in this article, the observations show that the latter may be weakened strikingly over a specific height range such that the former could be fairly greater than those due to refractivity fluctuations by about 15 dB, provided a strong updraft exists in the precipitating atmosphere. With employing the effect of the negative temperature-humidity covariance on the magnitude of variance of refractivity fluctuations, which can be attributed to the effects of decrease of water vapor through condensation process and the cooling of air parcel due to the saturated-adiabatically lifted-up, the depletion of turbulent echo powers in precipitating environment can thus be explained.

Acknowledgment

This work is partially supported by National Science Council (NSC) of Taiwan, Republic of China, under the grant NCU82-0202-M008-56.

Reference

Atlas, D., R.C.Srivastava, and R.S.Sehon, Doppler radar characteristics of precipitation at vertical incidence, Rev. Geophys., Vol.11, P.1-35, 1973

Balsley, B. B., and K.S.Gage, The MST radar techniques : Potential for middle atmosphere studies, Pure and Applied Geophys., Vol.118, P.452-493, 1980

Battan, L.J., Radar observation of the atmosphere, University of Chicago Press,324pp, 1973

Bean, B.R., and E.J.Dutton, Radio meteorology, U.S.Government Printing Office, Washington, D.C., 431pp, 1966

Chu, Y.H., J.K.Chao, C.H.Liu, and J.Rottger, Aspect sensitivity at tropospheric heights measured with vertically pointed beam of the Chung-Li VHF radar, Radio Sci., Vol.25, P.539-550, 1990

Doviak, R.J., and D.S.Zrnic, Doppler radar and weather observations, 458pp, Academic Press, Troy, Mass., 1984

Fletcher, N.H., The physics of raincloud, 386pp, Cambridge University Press, NewYork, 1972

Fukao, S.K., K.Wakasugi, T.Sato, S.Morimoto, T.Tsuda, I.Hirota, I.Kimura, andS.Kato, Direct measurement of air and precipitation particle motion by VHF Dopplerradar, Nature, 316, P.712-714, 1985

Gage, K.S., W.L.Ecklund, A.C.Riddle, and B.B.Balsley, Objective tropopause heightdetermination using low-resolution VHF radar observations, J. Atmos. Oceanic Technol., Vol.3, P.248-254, 1986

Gossard, E.E., and R.G.Strauch, Radar observation of clear air and cloud, Elsevier Science Publishers, 280pp, 1983

Larsen, M.F., and J.Rottger, Observations of thunderstorm reflectivities and Dopplervelocities measured at VHF and UHF, J. Atmos. Oceanic Technol. P.151-159, 1987

Masuda,Y, Influence of wind and temperature on the height limit of a radio acoustic sounding system, Radio Sci., Vol.23, P.647-654, 1988

Rottger, J., C.H.Liu, J.K.Chao, A.J.Chen, Y.H.Chu, I.J.Fu, C.M.Huang, Y.W.Kiang, F.S.Kuo, C.H.Lin, and C.J.Pan, The Chung-Li VHF radar: Technical layout and a summary of initial results, Radio Sci., Vol.25, P.487-502, 1990

Szoke, E.J., and E.J.Zipser, A radar study of convective cells in mesoscale systems in GATE, part I, Vertical profile statistics and comparison with hurricanes, J. Atmos. Sci., Vol.43, P.182-197, 1986

Tatarskii, V.I., Wave propagation in a turbulent media, McGraw-Hill, New York, 285pp,1961

Wakasugi, K., S.Fukao, S.Kato, A.Q.Mizutani, and M.Matsuno, Air and precipitation particle motions within a cold front measured by the MU radar, Radio Sci., Vol.20,P.1233-1240, 1985

Wakasugi, K., A.Mitsutani, M.Matsuno, S.Fukao, and S.Kato, A direct method for deriving drop-size distribution and vertical air velocities from VHF Doppler radar spectra, J. Atmos. Oceanic Technol., Vol.3, P.623-629, 1986

Wakasugi, K., A.Mizutani, M.Matsuno, S.Fukao, and S.Kato, Further discussion onderiving drop-size distribution and vertical air velocities directly from VHF doppler radar spectra, J. Atmos. Oceanic Techno., P.170-179, 1987

Wallace,J.M., and P.V.Hobbs, Atmospheric science: An introductory survey, Academic Press, 467pp, 1977

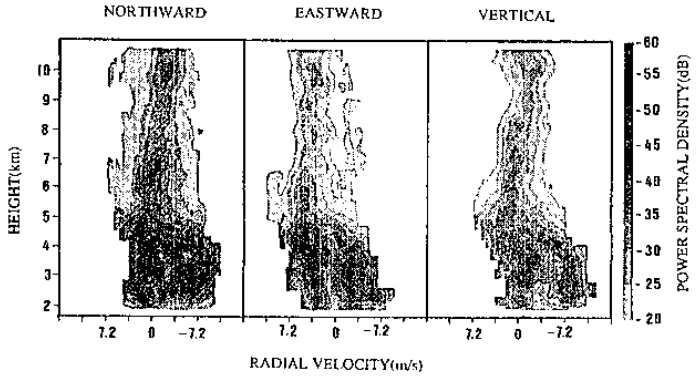

Fig.1a The echo power contour plots of Doppler spectra associated with precipitation for the radar beams pointed toward vertical, eastward, and northward, respectively, are shown. The spectra are obtained around 0910LT and averaged about 2.1 minutes. Two remarkable spectral peaks are occurred in each panel, one is responsible for precipitation echoes, the other one is identified as turbulent returns. As illustrating in the text.

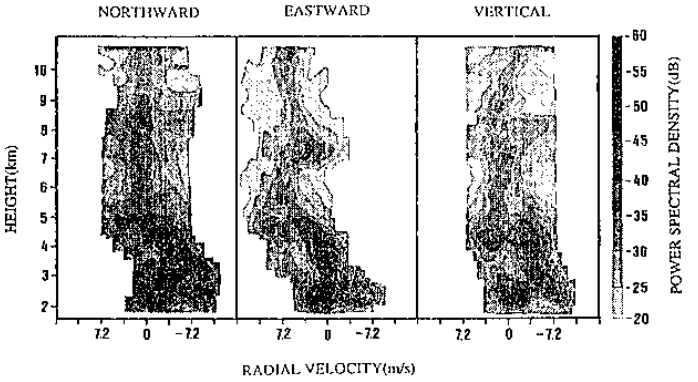

Fig.1b Same as Fig.1a, but the observational time is about 0927LT.

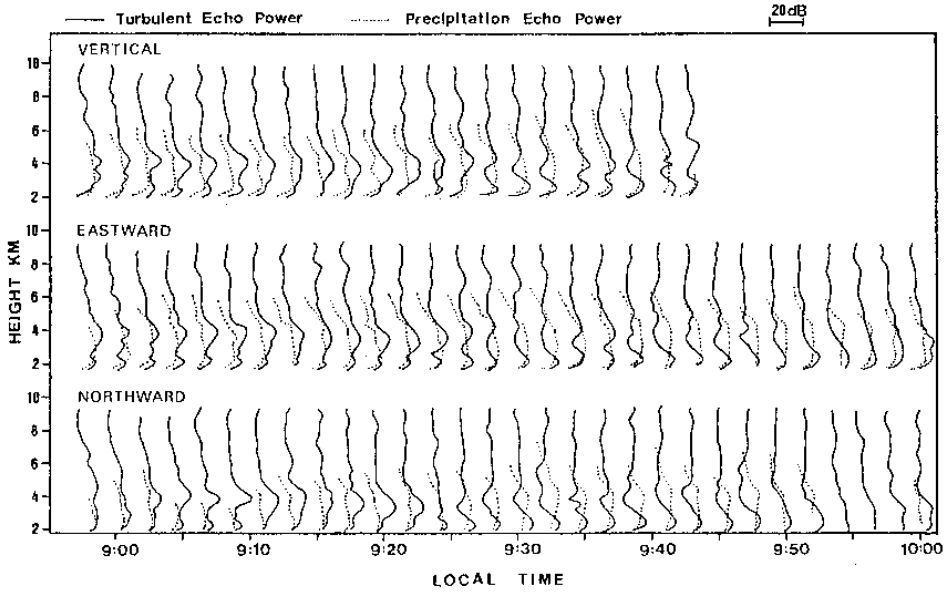

Fig.2 The height-time distributions of the echo power profiles for the atmospheric refractivity fluctuations (solid lines) and the hydrometeors (dotted lines), respectively, for the different pointing directions of radar beams.

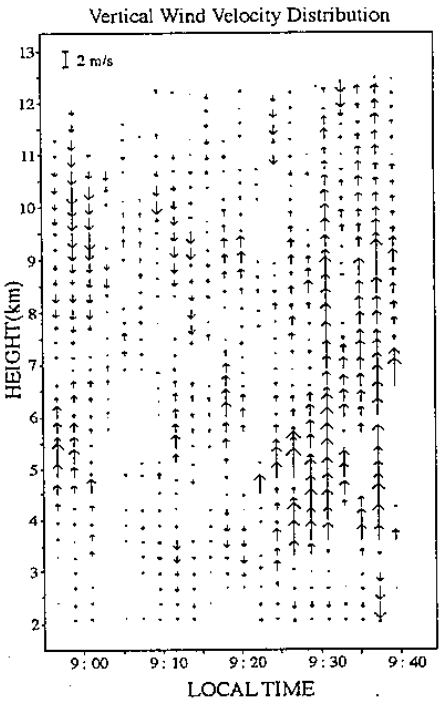

Fig.3 The height-time variations of the vertical wind velocity.

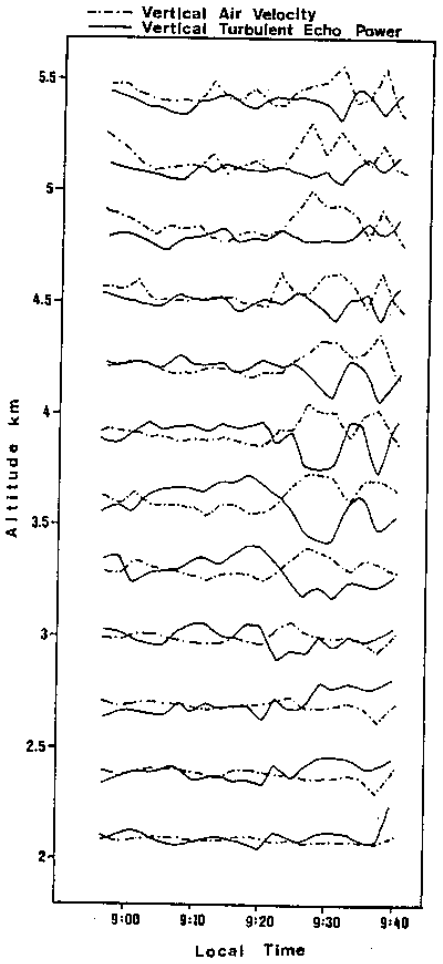

Fig.4 The comparing of the vertical wind speeds (solid lines) with the turbulent echo powers (dash-dotted lines) observed by using vertically pointed radar beams.

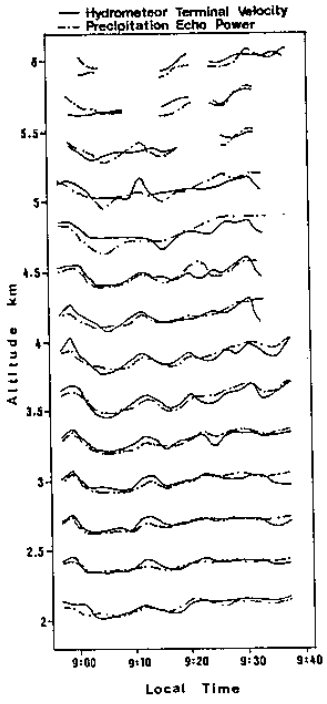

Fig.5 The comparing of the rain drop terminal velocity (solid lines) and the vertical radar echo powers (dash-dotted lines) scattered from rain drops.

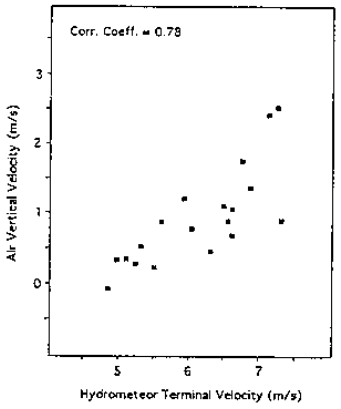

Fig.6 The scatter diagram of vertical wind speed v.s. hydrometeor terminal velocity averaged over the height range 3 km to 5 km.

以中壢VHF雷達對降雨環境之亂流回波功率的觀測與研究

朱延祥與林仲賢

國立中央大學太空科學研究所

摘要

根據過去國內外不同之VHF雷達對降水大氣的觀測顯示，在溶解層以下的高度範圍中，由降水顆粒所產生的雷達回波強度，一般均比由大氣折射指數不規則擾動散射的雷達回波功率要弱約20-30 dB。然而在本論文中，根據中壢VHF雷達的觀測結果，吾人將證實在溶解層以下的2-5公里的高度範圍內，前者的回波功率在適當的條件下有可能高於後者達15 dB以上。詳細的檢視及比較降水顆粒以及大氣折射指數回波功率的剖面圖，以及相關的降水與大氣的速度隨高度的變動情形，發現大氣折射指數回波功率在降水大氣中的急遽衰減係與大氣的強勁上升氣流有關。進一步的分析顯示，當大氣折射指數回波功率急遽減少時，雨滴終端速度與降雨回波功率呈現明顯的正相關，而垂直風速與亂流回波功率則顯現負相關的關係。根據這些觀測結果，在本論文中將提出一個可能的降水顆粒與背景大氣之交互作用的過程，以解釋前述的觀測現象。